

# 5th Japan Astronomy Olympiad National Finals

## Practical Problems

February 22, 2026 16:15–17:45

### Instructions

1. Do not open this problem booklet until instructed to begin.
2. This booklet contains 12 pages in total. If any pages are missing, out of order, or have unclear printing, raise your hand and notify the proctor.
3. Use only a black pencil or black mechanical pencil for all answers.
4. Write your examinee number in the designated field on the answer sheet and answer graph sheet. Do not write your examinee number anywhere else.
5. Write your answers only in the designated areas of the answer sheet and answer graph sheet.
6. Do not write any irrelevant characters, symbols, or marks in the answer areas.
7. For numerical answers where significant figures are not specified, use your own judgment to round to an appropriate number of significant figures. Answers with too many or too few significant figures may be penalized.
8. The margins of this booklet may be used for scratch work, but do not tear any pages.
9. Do not take the answer sheet or answer graph sheet home.
10. After the exam ends, take the problem booklet, calculation paper, and draft paper home.
11. Questions about the problems will not be answered. If you believe there is an error in a problem, note it on the answer sheet; it will be taken into consideration during grading.

## Problem 1 (50 points)

Answer the following questions (Questions 1–4) about various aspects of astronomical observation. For questions specified on the answer sheet, write the formulas and reasoning that lead to your answer. The observation location for all questions is longitude  $135^\circ\text{E}$ , latitude  $35^\circ\text{N}$ , and azimuth is measured from north toward east.

Figure 1–1 is an all-sky star chart observed at 20:00 JST (Japan Standard Time) on a certain day. The local sidereal time at longitude  $135^\circ\text{E}$  at this time is 23h 18m. Some solar system objects have been omitted from this star chart.

Answers to the following questions should be marked on the figure on the answer sheet.

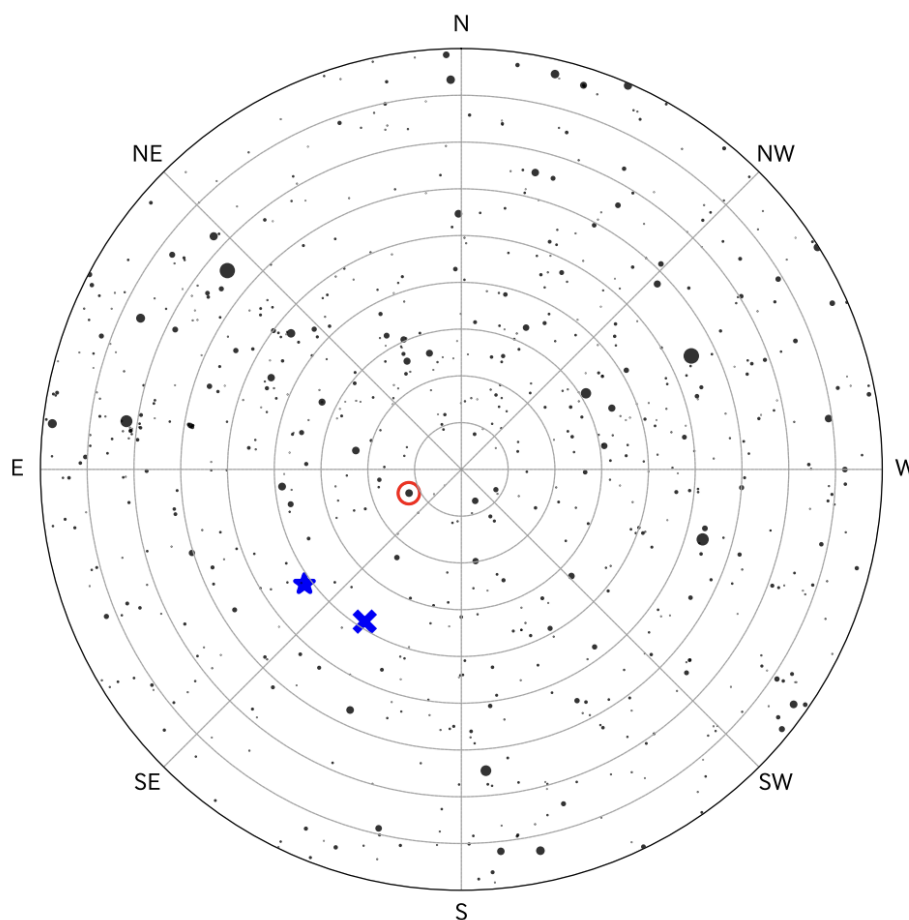


**Figure 1–1:** The night sky observed from longitude  $135^\circ\text{E}$  at 20:00 JST on a certain day. Lines indicating altitude and azimuth are drawn. Cardinal directions N, NE, E, SE, S, SW, W, NW are marked. A red circle ( $\odot$ ) marks one stellar object near the centre; a blue star ( $\star$ ) and blue cross ( $\times$ ) mark the positions of planet X observed one year apart.

### Question 1

- (1) In Figure 1–1, give the proper name and Bayer designation of the object marked with the red circle ( $\odot$ ).

- (2) On the star chart on the answer sheet (identical to Figure 1–1), mark with a  $\times$  symbol the approximate positions of the following Messier objects. Write the name of each object (M1, etc.) next to each mark.

**M1, M31, M36**

### Question 2

On the star chart on the answer sheet, draw the Galactic plane (the line of Galactic latitude  $b = 0^\circ$ ) as a solid line.

### Question 3

An observer wishes to observe the constellation *Sagitta* (the Arrow), located near the Summer Triangle, using binoculars.

- (1) On the star chart on the answer sheet, circle **exactly one** star belonging to Sagitta.
- (2) What is the minimum true field of view (in degrees) that the binoculars must have in order to fit all four of the brightest stars of Sagitta within the field of view simultaneously? Give your answer to 1 significant figure. An answer up to 1.5 times the minimum field of view is acceptable.

### Question 4

- (1) The object marked with the blue  $\times$  in Figure 1–1 is a solar system planet X. When planet X was observed one year later at the same date and time, it appeared at the position marked with the blue  $\star$ . Choose the most appropriate identification for planet X from the options below, and estimate its orbital period in years.

**Mars      Saturn      Uranus      Neptune**

- (2) Find the altitude of planet X at upper culmination (meridian transit) on the observation date. For simplicity, assume that the altitude of planet X (blue  $\times$ ) at the time of observation in Figure 1–1 is  $50^\circ$  and its azimuth is  $150^\circ$ .
- (3) Find the local sidereal time at the moment planet X transits the meridian on the observation date.

## Problem 2 (50 points)

Answer the following questions (Questions 1–6) about the characteristics of instruments used in astronomical observation and the quality of the data obtained.

When acquiring data with a detector to observe celestial objects, the data contain not only the signal from the object but also noise arising from various sources. If the noise is much stronger than the signal, the signal is buried in the noise and the object cannot be detected. To quantify detectability, the *signal-to-noise ratio* (S/N ratio) is used: it is the signal strength  $S$  divided by the noise strength  $N$ .

In the following problems, unless otherwise noted, let  $I$  be the brightness of the object,  $t$  the exposure time, and  $w$  the observation wavelength bandwidth.  $S$  is proportional to  $I \times t \times w$ , and only Poisson noise from the background light (brightness  $B$ ) is considered, with  $N$  proportional to  $\sqrt{B \times t \times w}$ .

### Question 1

To what power of exposure time  $t$ , and to what power of wavelength bandwidth  $w$ , is the S/N ratio proportional? Answer for each.

### Question 2

In a certain optical system, a 12th-magnitude star observed for 1 second through a filter of bandwidth 100 nm and transmittance 1.0 gave S/N = 10. The background brightness is assumed constant.

- (1) Using the same settings, find the exposure time required to achieve S/N = 20 for a 15th-magnitude star.
- (2) Starting from the settings in (1), the filter is changed to a narrowband filter with bandwidth 10 nm and transmittance 0.8. Find the exposure time required to achieve S/N = 20 for the 15th-magnitude star with this new filter.

### Question 3

A total exposure time  $T$  is divided into  $n$  equal sub-exposures, each captured as a separate image; the  $n$  images are then combined into one.

- (1) If the signal in the combined image is  $n$  times that of a single image and the noise is  $\sqrt{n}$  times, compare the S/N ratio of the combined image with the S/N ratio of a single exposure of full duration  $T$ .
- (2) In actual observations, in addition to Poisson noise, there is a type of noise called *read noise* that does not depend on exposure time. If the total noise per frame is  $\sqrt{N_{\text{Poisson}}^2 + R^2}$  (where  $R$  is the read noise), explain from the perspective of the S/N ratio why dividing the total exposure into many short sub-exposures is disadvantageous.

### Question 4

A photometric observation of a celestial object was performed. When the brightness profile of the stellar image (the distribution of count values per pixel) was examined in the obtained image data, the peak region — which should normally be bell-shaped — appeared flattened horizontally at a constant value, as shown in Figure 2–1. Explain why this phenomenon occurs, from the perspective of the physical characteristics of the detector.

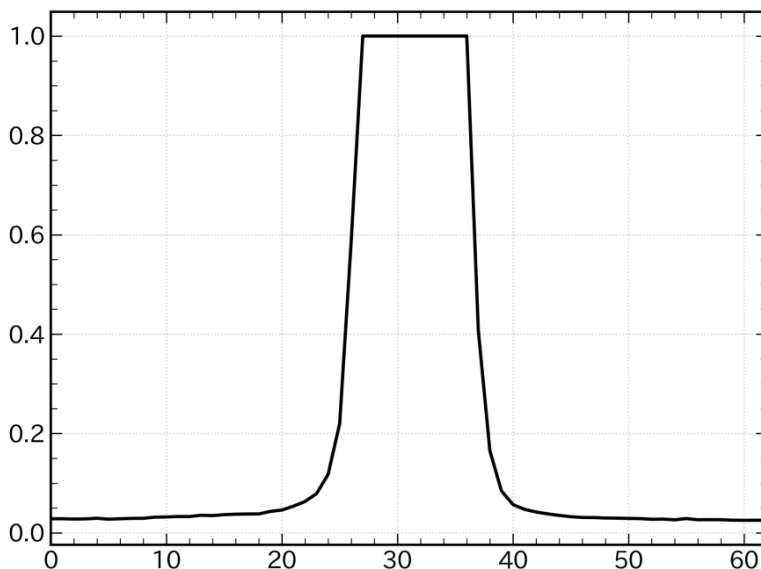


**Figure 2–1:** Brightness profile of a stellar image. Horizontal axis: pixel number (0–60); Vertical axis: normalized count value (0.0–1.0). The profile is flat-topped (saturated) between approximately pixels 25–38 instead of showing the expected smooth bell curve.

### Question 5

Aside from avoiding the phenomenon described in Question 4, what advantages does compositing multiple short-exposure images have compared to taking a single long-exposure image? Answer briefly.

In astronomical observations using a cooled CCD camera, a calibration process called *primary reduction* (basic image reduction) is required to remove detector and optical-system effects so that the true physical brightness of the object can be recovered. Primary reduction uses the object images together with the following separately acquired calibration frames:

**Light frame:** The raw image of the astronomical object taken through the telescope. In addition to the object’s light, it contains detector-derived noise and non-uniformity from the optical system.

**Dark frame:** An image taken with the telescope capped, using the same exposure time and temperature as the light frame. Only detector-derived noise is recorded.

**Flat frame:** An image of a uniformly bright light source. It records optical effects such as “vignetting” (peripheral darkening) from lenses and mirrors. The flat frame has normally been pre-processed with a dark frame and its brightness is normalised to 1.

**Question 6**

Using a certain  $4 \times 4$ -pixel detector, light, dark, and flat frames were captured, yielding the values shown below. Using these data, calculate the corrected value for each pixel and fill in the  $4 \times 4$  grid on the answer sheet.

$$\text{Corrected value} = \frac{\text{Light} - \text{Dark}}{\text{Flat}}$$

**Light Frame**

55	79	65	37
74	96	80	43
58	81	53	29
25	33	24	19

**Dark Frame**

3	8	1	5
9	2	7	4
6	1	10	2
5	4	3	8

**Flat Frame**

0.9	1	1	0.9
1	1.1	1.1	1
1	1.1	1.1	1
0.9	1	1	0.9

### Problem 3 (100 points)

In recent years, advances in observational technology have rapidly accelerated the exploration of distant galaxies, deepening our understanding of the early universe. Answer the following questions (Questions 1–2) while performing data analysis on distant-galaxy surveys and their statistics. In this problem, the **AB magnitude system** is used.

#### Question 1

Read the following passage about the Lyman- $\alpha$  break — an important spectral feature in distant-galaxy surveys — and answer the questions below.

The *Lyman series* is the collective name for line spectra arising from electron transitions between energy levels  $n \geq 2$  and  $n = 1$  in the hydrogen atom ( $n$  is the principal quantum number). The line from the  $n = 2 \rightarrow n = 1$  transition is called the *Lyman- $\alpha$  line*. When UV radiation passes through a gas cloud rich in neutral hydrogen, a Lyman- $\alpha$  absorption line is produced because photons are used to excite hydrogen from  $n = 1$  to  $n = 2$ . At wavelengths (A) than Lyman- $\alpha$ , discrete Lyman absorption lines arise from excitation of  $n = 1$  hydrogen to  $n \geq 3$  levels. The wavelength corresponding to the  $n = \infty$  (complete ionisation)  $\rightarrow n = 1$  transition is called the *Lyman limit*; at wavelengths (B) than the Lyman limit, continuous absorption occurs due to ionisation of neutral hydrogen.

As UV radiation from high-redshift galaxies travels to us, Lyman- $\alpha$  absorption by foreground intergalactic neutral hydrogen at various redshifts is dominant, so light shortward of Lyman- $\alpha$  is almost entirely absorbed. Consequently, high-redshift galaxy spectra show a characteristic sharp drop in energy flux density at the Lyman- $\alpha$  wavelength toward shorter wavelengths. This feature is called the *Lyman- $\alpha$  break*.

The *dropout technique* exploits the Lyman- $\alpha$  break to search for distant galaxies: photometric observations with multiple filters are used to capture the Lyman- $\alpha$  break between two adjacent filters, selecting candidate objects at a specific redshift range. Galaxy spectra can also exhibit a *Balmer break*, arising at the wavelength corresponding to the  $n = \infty \rightarrow n =$  (C) transition. In dropout surveys, care must be taken not to confuse the Balmer break of a galaxy at (D) redshift with the Lyman- $\alpha$  break.

- (1) Fill in blanks **(A)**, **(B)**, **(C)**, and **(D)** in the passage above with the appropriate words or values.
- (2) When an electron in a hydrogen atom transitions between energy levels  $n_1$  and  $n_2$  ( $n_1 < n_2$ ), the wavelength  $\lambda$  of the resulting line spectrum follows the Rydberg formula:

$$\frac{1}{\lambda} = R_{\infty} \left( \frac{1}{n_1^2} - \frac{1}{n_2^2} \right), \quad R_{\infty} = 1.09737 \times 10^7 \text{ m}^{-1}.$$

Using this formula, find the wavelengths of the Lyman- $\alpha$  line and the Lyman limit in nm to 4 significant figures.

- (3) Figure 3–1 shows the JWST spectrum of a galaxy in which the Lyman- $\alpha$  break is prominent. Find the redshift of this galaxy.
- (4) A survey of distant galaxies was conducted using the dropout technique with JWST NIRCcam multi-filter photometry. A galaxy candidate with the spectral energy distribution (SED) shown in Figure 3–2 was found. Assuming the observed sharp

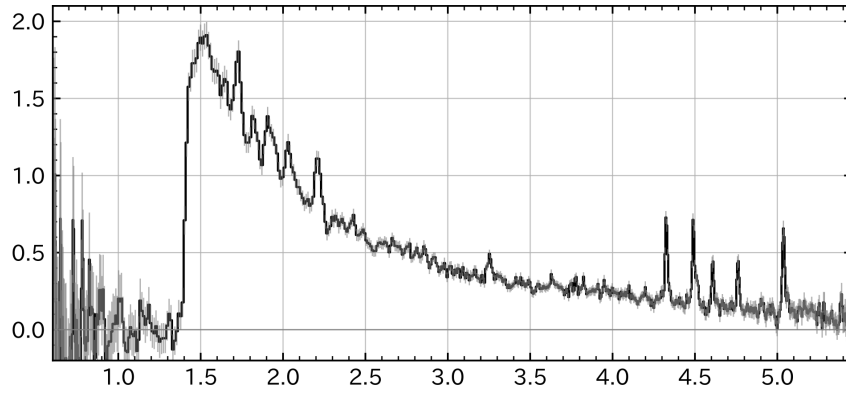


**Figure 3–1:** Spectrum of a galaxy with a prominent Lyman- $\alpha$  break. Horizontal axis: observed wavelength  $\lambda / \mu\text{m}$  (1.0–5.0); Vertical axis: energy flux density  $/10^{-20} \text{ erg s}^{-1} \text{ cm}^{-2} \text{ \AA}^{-1}$  (0.0–2.0). The flux drops sharply to near zero below  $\sim 1.4 \mu\text{m}$ . Data from JADES DR4 (Curtis-Lake et al. 2025, arXiv:2510.01033), doi:10.17909/8tdj-8n28.

change in magnitude is due to the Lyman- $\alpha$  break, select the most appropriate redshift for this galaxy from the options below. Briefly state your reasoning.

- ①  $z = 8$       ②  $z = 10$       ③  $z = 12$       ④  $z = 14$

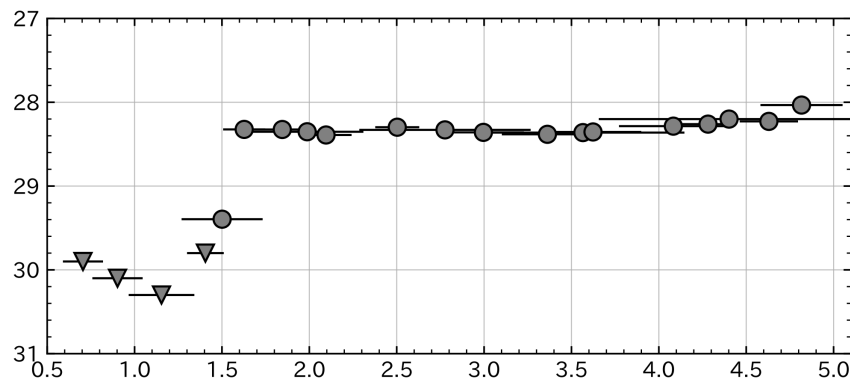


**Figure 3–2:** SED of a distant-galaxy candidate found by the dropout technique. Horizontal axis: observed wavelength  $/ \mu\text{m}$  (0.5–5.0); Vertical axis: AB magnitude (27–31, inverted). Circle (o) points are detections; downward-triangle ( $\nabla$ ) points are upper limits (non-detections). Horizontal error bars show the wavelength range of each filter. The galaxy is undetected below  $\sim 1.5 \mu\text{m}$  and detected at  $\sim 28$  mag above.

## Question 2

Galaxies are the sites of star formation and chemical evolution in the universe. Understanding how the number density of galaxies changes with redshift — the cosmic evolution of galaxy number density — is important. Because number density depends on luminosity (more luminous galaxies are rarer), the *luminosity function*  $\Phi(M_{\text{UV}})$  [ $\text{Mpc}^{-3} \text{mag}^{-1}$ ] is used when comparing number densities at different redshifts. It gives the number density per unit absolute magnitude as a function of UV absolute magnitude  $M_{\text{UV}}$ .

Figure 3–3 shows an example UV luminosity function: galaxies brighter in UV (smaller  $M_{\text{UV}}$ ) have lower number densities.

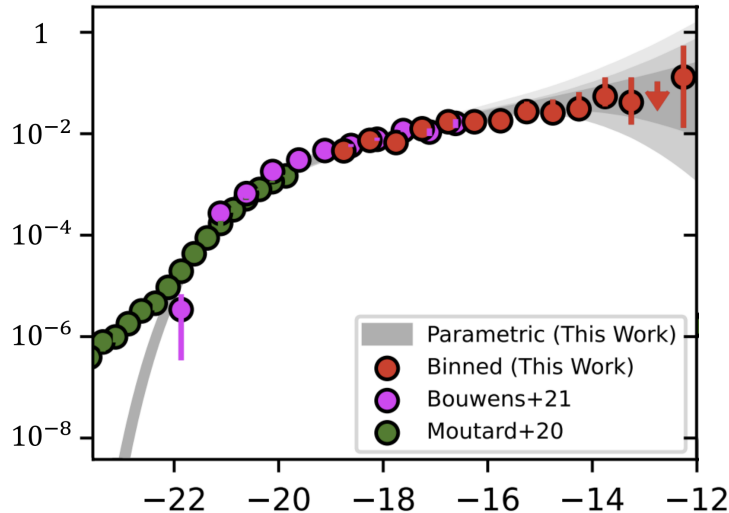


**Figure 3–3:** Example UV luminosity function from Bouwens et al. (2022), *ApJ*, 940, 55, at  $z \sim 2$ . Horizontal axis:  $M_{\text{UV}}$  ( $-22$  to  $-12$ ); Vertical axis:  $\Phi(M_{\text{UV}})/\text{Mpc}^{-3} \text{mag}^{-1}$  (log scale,  $10^{-8}$  to 1).

In this question we compute and plot the UV luminosity function from galaxy counts found by the dropout technique. Using filters that select  $z = 5.5$ – $6.5$  galaxies, distant galaxies were selected from a  $1.0 \text{deg}^2$  field. Table 3–1 gives the number of galaxies in each  $M_{\text{UV}}$  bin.

**Table 3–1:** Number of  $z = 5.5$ – $6.5$  dropout-selected galaxies per  $M_{\text{UV}}$  bin.

$M_{\text{UV}}$ bin	Count	$M_{\text{UV}}$ bin	Count
$-23.0 \sim -22.5$	2	$-21.0 \sim -20.5$	969
$-22.5 \sim -22.0$	27	$-20.5 \sim -20.0$	2039
$-22.0 \sim -21.5$	110	$-20.0 \sim -19.5$	3792
$-21.5 \sim -21.0$	461	$-19.5 \sim -19.0$	6244

- (1) Find the volume of the survey region in  $\text{Mpc}^3$  to 2 significant figures. The comoving distances to  $z = 5.5$  and  $z = 6.5$  are  $8.02 \times 10^3 \text{Mpc}$  and  $8.44 \times 10^3 \text{Mpc}$  respectively. You may use the fact that the full sky subtends  $41253 \text{deg}^2$ .
- (2) By dividing the number of objects per unit magnitude bin by the survey volume, find  $\Phi(M_{\text{UV}})$  at  $z = 5.5$ – $6.5$  in units of  $\text{Mpc}^{-3} \text{mag}^{-1}$ . Assuming Poisson statistics, take the uncertainty in a count  $N$  to be  $\sqrt{N}$ , and propagate this to obtain the

uncertainty in the luminosity function. Present your results in the format “value  $\pm$  uncertainty” in the table on the answer sheet.

[Note: In practice, corrections for completeness and contamination (e.g. Balmer-break interlopers) are applied. For simplicity, treat the counts in Table 3–1 as already corrected.]

- (3) Using the results of (2), plot  $\Phi(M_{UV})$  on answer graph sheet ① (semi-log,  $M_{UV}$  on the linear axis). Show the uncertainties from (2) as vertical error bars, use the bin midpoint as the horizontal coordinate, and indicate the bin width with horizontal error bars. Figure 3–4 shows an example of how to draw such a graph.

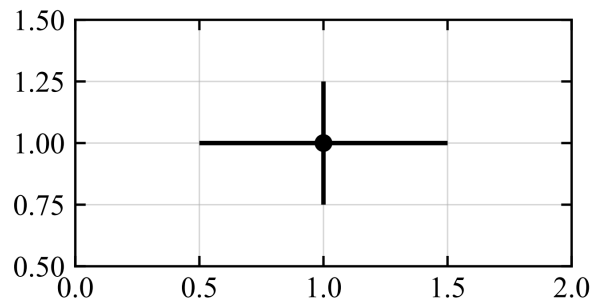


**Figure 3–4:** Example of a data point with error bars for Question 2(3). The point is at  $x = 1$  (bin 0.5–1.5),  $y = 1$ , with a  $y$ -direction uncertainty of 0.25.

- (4) When the AB magnitude system is used, the apparent magnitude  $m$  and the energy flux density per unit frequency  $f_\nu$  satisfy

$$f_\nu = 3.631 \times 10^{-0.4m} \times 10^{-20} \text{ erg s}^{-1} \text{ cm}^{-2} \text{ Hz}^{-1}.$$

Show that the absolute magnitude  $M$  and luminosity per unit frequency  $L_\nu$  satisfy

$$L_\nu = 4.34 \times 10^{-0.4M} \times 10^{20} \text{ erg s}^{-1} \text{ Hz}^{-1}.$$

Use  $1 \text{ pc} = 3.09 \times 10^{18} \text{ cm}$ .

- (5) Using the results of (2), compute the UV luminosity density at  $z = 5.5\text{--}6.5$ :

$$\rho_{UV} = \sum_{M_{UV}=-23}^{-19} L_{\nu,UV} \times \Phi(M_{UV}) \times \Delta M_{UV} \quad [\text{erg s}^{-1} \text{ Hz}^{-1} \text{ Mpc}^{-3}].$$

Treat  $\Phi$  as constant within each bin. Evaluate  $L_{\nu,UV}$  using the formula in (4) at the bin midpoint. No uncertainty estimate is required.

- (6) UV radiation from galaxies is dominated by short-lived massive stars, so the star formation rate (SFR [ $M_\odot \text{ yr}^{-1}$ ]), averaged over  $\sim 10 \text{ Myr}$ , is related to  $L_{\nu,UV}$  by

$$\text{SFR} = 1.4 \times 10^{-28} \left( \frac{L_{\nu,UV}}{\text{erg s}^{-1} \text{ Hz}^{-1}} \right) M_\odot \text{ yr}^{-1}.$$

Using this relation, convert the UV luminosity density  $\rho_{UV}$  in Table 3–2 for each redshift bin into a SFR density [ $M_\odot \text{ yr}^{-1} \text{ Mpc}^{-3}$ ] and fill in the table on the answer sheet. For the  $z = 5.5\text{--}6.5$  bin use the  $\rho_{UV}$  obtained in (5).

**Table 3–2:** UV luminosity density  $\rho_{UV}$  by redshift bin.

$z$ bin	$\rho_{UV}$ [ $\text{erg s}^{-1} \text{ Hz}^{-1} \text{ Mpc}^{-3}$ ]	$z$ bin	$\rho_{UV}$ [ $\text{erg s}^{-1} \text{ Hz}^{-1} \text{ Mpc}^{-3}$ ]
0.1 ~ 0.3	$7.6 \times 10^{25}$	2.3 ~ 2.7	$3.6 \times 10^{26}$
0.3 ~ 0.5	$1.1 \times 10^{26}$	2.7 ~ 3.1	$3.0 \times 10^{26}$
0.5 ~ 0.7	$1.6 \times 10^{26}$	3.1 ~ 3.5	$2.4 \times 10^{26}$
0.7 ~ 1.1	$2.4 \times 10^{26}$	3.5 ~ 4.5	$1.7 \times 10^{26}$
1.1 ~ 1.5	$3.4 \times 10^{26}$	4.5 ~ 5.5	$1.0 \times 10^{26}$
1.5 ~ 1.9	$4.1 \times 10^{26}$	5.5 ~ 6.5	<i>(from (5))</i>
1.9 ~ 2.3	$4.1 \times 10^{26}$	6.5 ~ 7.5	$4.4 \times 10^{25}$
		7.5 ~ 8.5	$3.2 \times 10^{25}$

- (7) Using the results of (6), plot the cosmic SFR density as a function of redshift on answer graph sheet ② ( $z$  on the horizontal axis, SFR density on the vertical axis). Use the bin midpoint as the horizontal coordinate and indicate the bin width with horizontal error bars. No vertical error bars are required. Also state to 1 significant figure the redshift at which the SFR density peaks (i.e. the epoch of most active star formation in the universe). If no graph is provided, no credit will be given for the redshift answer.